Correlation between the Activities and the Oligomeric Forms of Pig Gastric H/K-ATPase†

Kazuhiro Abe,‡ Shunji Kaya,‡ Yutaro Hayashi,§ Toshiaki Imagawa,‡ Mahito Kikumoto,|| Kazuhiro Oiwa,|| Tsuyoshi Katoh,⊥ Michio Yazawa,▽ and Kazuya Taniguchi*,‡

Biological Chemistry and Bioorganic Chemistry, Division of Chemistry, Graduate School of Science, Hokkaido University, Sapporo 060-0810, Department of Biochemistry, Kyorin University School of Medicine, Mitaka 181-1611, Communications Research Laboratory, Kansai Advanced Research Center, Kobe 651-2492, and Department of Biochemistry, Asahikawa Medical College, Asahikawa 078-8510, Japan

Received September 18, 2003; Revised Manuscript Received October 22, 2003

ABSTRACT: Membrane-bound H/K-ATPase was solubilized by octaethylene glycol dodecyl ether ($C_{12}E_8$) or *n*-octyl glucoside (nOG). H/K-ATPase activity and the distribution of protomeric and oligomeric components were evaluated by high-performance gel chromatography (HPGC) and by single-molecule detection using total internal reflection fluorescence microscopy (TIRFM). As evidenced by HPGC of the $C_{12}E_8$-solubilized enzyme, the distribution of oligomers was 12% higher oligomeric, 44% diprotomeric, and 44% protomeric species, although solubilization by $C_{12}E_8$ reduced the H/K-ATPase activity to 1.8% of that of the membrane-bound enzyme. The electron microscopic images of the $C_{12}E_8$-solubilized enzyme showed the presence of protomers and a combination of two and more protomers. While the nOG-solubilized H/K-ATPase retained the same turnover number and 71% of the specific activity as that of the membrane-bound enzyme, 56% higher oligomeric, 34% diprotomeric, and 10% protomeric species were detected. TIRFM analysis of solubilized fluorescein 5′-isothiocyanate (FITC)-modified H/K-ATPase at Lys-518 of the α-chain showed a quantized photobleaching of the FITC fluorescence intensity. For the $C_{12}E_8$-solubilized FITC−enzyme, the fraction of each of the initial relative fluorescence intensity units of 4, 2, and 1 was, respectively, 5%, 44% and 51%. In the case of the nOG-solubilized FITC−enzyme, each fraction of 4 and 2 units was, respectively, 54% and 46% with no detectable 1 unit fraction. This represents the first direct observation of H/K-ATPase in aqueous solution. The correlation between the enzymatic activities and distribution of oligomeric forms of H/K-ATPase by HPGC and the observation of a single molecule of H/K-ATPase and others suggests that the tetraprotomeric form of H/K-ATPase molecules represents the functional species in the membrane.

The transport of H^+ and K^+ coupled hydrolysis of ATP is performed by H/K-ATPase[1] (*1*−*3*). The enzyme has been shown to be composed of an α (catalytic)-chain and a *β*-chain, the latter of which plays a role in membrane insertion and traffic (α*β*-protomer). The catalytic subunits of P-type ATPases, such as gastric H/K-ATPase, Na/K-ATPase, and sarcoplasmic Ca/H-ATPase, have homologous primary structures (*4*−*6*). High-resolution monomeric crystal structures of Ca/H-ATPase have recently been reported, which permits an assessment of interdomain interactions during ATP hydrolysis (*7*, *8*). However, a large body of evidence has accumulated to indicate that the functional native enzyme in the membrane is an oligomer comprised of α*β*-protomers in H/K-ATPase (*9*−*17*) and Na/K-ATPase (*16*, *18*−*28*) or a 2*n*-mer in sarcoplasmic Ca/H-ATPase (*29*−*31*). In the case of H/K-ATPase, the following data provide strong support for the oligomericity of the enzyme: studies of radiation inactivation (*10*), stoichiometry of phosphorylation and ATP binding (*12*) E3810 (rabeprazole) binding (*14*), chemical cross-linking with copper orthophenanthroline (*13*), blue-native polyacrylamide electrophoresis (*15*), a glycerol density gradient of detergent-extracted enzyme (*9*), and two-dimensional crystals (*11*). We recently showed that the maximum absolute amount of EP formed from ATP was 0.5 mol/mol of α-chain, which is half the amount of EP obtained from P_i or acetyl phosphate (*12*, *17*). The amount of the enzyme-bound ATP (EATP) during turnover was shown to be 0.5 mol/mol of α-chain ($K_{0.5}$ = ∼0.1 mM), and the maximum ATP binding capacity in the presence of 1,2-cyclohexylenedinitrilotetraacetic acid (CDTA) was 1 mol/mol of α-chain ($K_{0.5}$ = ∼0.1 mM). The breakdown of EP formed in the presence of ∼micromolar ATP, accumulating

† This work was supported, in part, by Grants-in-Aid for Scientific Research (10308028 (to K.T.), 13142201 and 13680703 (to S.K.), and 15009844 (to K.A.)) from the Ministry of Education, Science, Sports, and Culture of Japan.

* To whom correspondence should be addressed. Phone and fax: +81-706-4245. E-mail: ktan@den.hokudai.ac.jp.

‡ Biological Chemistry, Hokkaido University.

§ Kyorin University School of Medicine.

|| Kansai Advanced Research Center.

⊥ Asahikawa Medical College.

▽ Bioorganic Chemistry, Hokkaido University.

[1] Abbreviations: H/K-ATPase, gastric potassium-activated adenosine triphosphatase; EP, phosphoenyzme; EATP, enzyme-bound ATP; P_i, inorganic phosphate; FITC, fluorescein 5′-isothiocyanate; HPGC, high-performance gel chromatography; TIRFM, total internal reflection fluorescence microscopy; $C_{12}E_8$, octaethylene glycol dodecyl ether; nOG, *n*-octyl glucoside.

10.1021/bi035686x CCC: $25.00
Published on Web 11/26/2003

EP:E, was more rapid than that in the presence of submillimolar ATP, thus permitting the accumulation of EP:EATP. One mole of P_i was simultaneously liberated from each 0.5 mol of EP and EATP (*12*, *17*). These data suggest that each catalytic α-chain is involved in cross-talk, thus maintaining half-site phosphorylation and half-site ATP binding, at least in the $(\alpha\beta)_2$-diprotomeric form of the enzyme, which appears to exclude the possibility of simultaneous phosphorylation and ATP binding to the same α-chain. Thus, for a better understanding of the mechanism of P-type ATPase, studies of the oligomericity of the enzyme would be highly desirable.

The aim of the present study was to determine the number of molecules associated with one another in the membrane-bound H/K-ATPase. Here we show evidence for the oligomeric nature of H/K-ATPase based on enzymatic activities, electron microscopic observation, high-performance gel chromatographic separation, and a single-molecule detection technique.

EXPERIMENTAL PROCEDURES

H/K-ATPase Preparation and FITC Modification. Methods have been described for the preparation of vesicles (G1 fraction) that contain pig gastric H/K-ATPase and their further purification by SDS (*32*, *33*). Purified H/K-ATPase preparations were stored in 0.25 M sucrose solutions containing 0.5 mM EGTA/Tris (pH 7.4) at − 80 °C until use. Protein concentrations were determined by the method of Bradford using bovine serum albumin as a standard (*34*). The methodology used for the determination of potassium-dependent ATPase activity and the amount of phosphoenzyme (EP) has been described previously (*12*, *17*). The specific activity of the purified enzyme was approximately 450 μmol of P_i/mg/h in a medium containing 25 mM sucrose, 0.1 mM EGTA/Tris, 40 mM HEPES/Tris, 10 mM KCl, 2 mM $MgCl_2$ and 2 mM ATP/Tris (pH 7.0) at 37 °C, and the EP from ATP in the absence of KCl was 2.5 nmol/mg at 25 °C. FITC modification of H/K-ATPase was performed as follows. H/K-ATPase preparations (0.5 mg/mL) were incubated in 1 mM EDTA, 100 mM Tris/HCl (pH 9.2), 0.25 M sucrose, and 10 μM of FITC/DMSO at 25 °C for 30 min. The modification was terminated by the addition of 1 mM β-mercaptoethanol, and the samples were washed twice with 10 mM HEPES/Tris (pH 7.0), 1 mM EDTA, and 0.25 M sucrose. To estimate the amount of enzyme-bound FITC, the FITC-modified H/K-ATPase preparations were incubated in a solution containing 1% (w/v) SDS and 100 mM Tris/HCl (pH 9.2) at room temperature for 1 h, and the absorbance at 495 nm (extinction coefficient 75000 M^{-1} cm^{-1} at 495 nm) was measured (*35*, *36*).

Detergent Solubilization of H/K-ATPase. The SDS-purified membrane-bound H/K-ATPase (2 mg/mL) was incubated in 0.6% (w/v) $C_{12}E_8$, 0.1 M CH_3COOK, 1 mM EDTA, 10% (w/v) glycerol, and 20 mM HEPES/Tris (pH 7.0) at 0 °C for 5 min. For solubilization by nOG, the purified H/K-ATPase (5 mg/mL) was incubated in a medium consisting of 20 mM MES/Tris (pH 5.5), 1 mM MgATP, 0.25 M sucrose, and 2% (w/v) nOG. The mixture was incubated for 5 min at 0 °C and then diluted with four volumes of the same buffer without added MgATP. For solubilization by SDS, the purified H/K-ATPase (2 mg/mL) was incubated in 1% (w/v) SDS, 0.1 M CH_3COONa, 0.25 M sucrose, and 20 mM HEPES/Tris (pH 7.0) at room temperature for 5 min. Each sample was centrifuged at 100000 rpm for 10 min (Optima TL, 100.2 rotor, Beckman) and the supernatant was collected. To determine the ATPase activities of detergent-solubilized H/K-ATPase at 25 °C, it was diluted with buffer containing 0.25 M sucrose and 20 mM MES/Tris (pH 5.5) at a final detergent concentration of less than 0.1%.

Electron Microscopic Observation of Rotary-Shadowed Molecules of H/K-ATPase. The procedure was essentially the same as that described previously (*25*). Samples of the H/K-ATPase preparation solubilized by $C_{12}E_8$ were diluted to around 10 μg/mL with 60% (w/v) glycerol, sprayed onto mica, rotary-shadowed with platinum, and observed with a Hitachi H-800 electron microscope operated at 75 kV.

Gel Chromatographic Separation of Solubilized H/K-ATPase. The solubilized H/K-ATPase preparations (200 μL) were subjected to HPGC (high-performance gel chromatography) with a TSKgel G3000SW_{XL} (7.8 × 300 mm, Tosoh) column equipped with a guard column (TSK guard column SW_{XL}, 6.0 × 40 mm). The column was equilibrated with buffer A for $C_{12}E_8$-solubilized H/K-ATPase, 0.03% (w/v) $C_{12}E_8$, 0.1 M CH_3COOK, 1 mM EDTA, 13 mM imidazole, 8 mM HEPES (pH 7.0), or buffer B for nOG-solubilized H/K-ATPase, 0.8% (w/v) nOG, 50 mM CholineCl, 1 mM EDTA, 3 mM $(CH_3COO)_2Mg$, 40 mM MES, 5 mM imidazole (pH 5.5). The samples were eluted at 0 °C at a flow rate of 0.35 mL/min. The elution profile of the protein (absorbance at 280 nm) was monitored with a diode array detector (SPD-M10AVP, Shimadzu). The solubilized H/K-ATPases were separated into four fractions: A (aggregate), H (higher oligomers), D (diprotomer), P (protomer).

Single-Molecule Observation. For single-molecule imaging, a flow cell was constructed with two coverslips (bottom, 24 × 36 mm^2; top, 18 × 18 mm^2) separated by two spacers of 50 μm (*37*). The samples solubilized by SDS, $C_{12}E_8$, and nOG were diluted to approximately 10 pM with buffers containing 0.1 M CH_3COOK, 0.1 M Tris/HCl (pH 8.5), and 2 mM $MgCl_2$ with the corresponding detergents (0.1% (w/v) SDS, 0.03% (w/v) $C_{12}E_8$, and 0.8% (w/v) nOG, respectively). An Olympus total internal reflection system (*38*) was used with minor modifications. An Ar^+ laser (model 532-A-A03, Melles Griot) was introduced to an inverted microscope (IX70, Olympus) through a single-mode fiber and two illumination lenses; the light was focused at the back focal plane of an objective lens (PlanApo60×OTIRFM; NA 1.45, Olympus). The power of the laser was 2.3 mW at the nose piece. The excitation beam was reflected at the glass surface and the sample solution, thus producing an evanescent field. Fluorescence images were collected through the objective lens and passed through a barrier filter (U-MNIBA, Olympus). Images were captured with a CCD video camera (CCD300-RC, DAGE MTI) coupled to an image intensifier (VS-1845, Video Scope International) and recorded on an S-VHS videotape using a frame rate of 30 Hz. The intensity and history of the fluorescent particles were analyzed using the Metamorph software program (version 4.6, Universal Imaging). For an analysis of histograms of the data and the calculation of rate constants, the Graphpad Prism software program (version 2.01) was used.

Chemicals. $C_{12}E_8$ was purchased from Nikko Chemical Co. nOG was purchased from Wako Chemicals Co. The

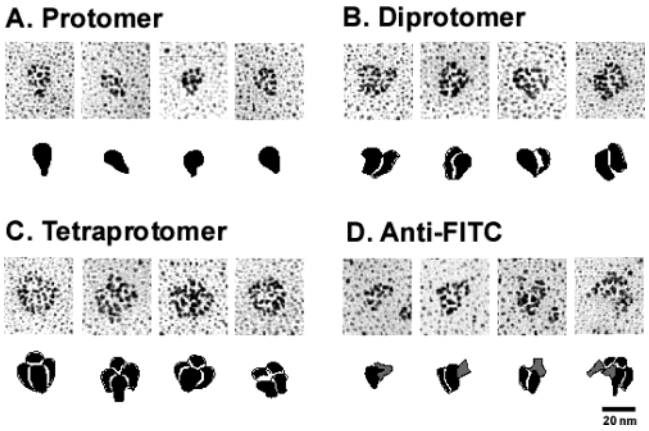

FIGURE 1: Gallery of selected electron micrographs of rotary-shadowed molecules. Samples of H/K-ATPase preparation solubilized by $C_{12}E_8$ were diluted with 60% glycerol, sprayed onto mica, rotary-shadowed with platinum, and observed with a Hitachi H-800 electron microscope. The H/K-ATPase molecules with protomeric (A), diprotomeric (B), and tetraprotomeric (C) appearance are shown. (D) FITC-modified H/K-ATPase complexed with anti-FITC antibody. The structure judged as most probable for its magnified image is drawn under each electron micrograph.

FITC and anti-FITC antibodies were purchased from Molecular Probes. All other chemicals were the highest grade available.

RESULTS

Electron Microscopic Observation of Rotary-Shadowed H/K-ATPase Molecules. A strong body of enzymological evidence exists to show the oligomericity of the enzyme, as described above. Thus, it should be possible to obtain morphological evidence for the oligomeric structure of H/K-ATPase by electron microscopy. An H/K-ATPase preparation, purified with SDS and solubilized with $C_{12}E_8$, was placed on a mica plate and rotary-shadowed with platinum. Figure 1 shows electron microscopic images of the spatially distributed individual $C_{12}E_8$-solubilized H/K-ATPase molecules. The protomeric image (Figure 1A) had a pearlike shape, approximately 18 nm in length and 12 nm in width at the widest portion. In addition to this protomeric image, images of combinations of two and more (3−4) protomers that are closely bound to each other were also observed (Figure 1B,C). To confirm that these images were derived from H/K-ATPase molecules, FITC-modified H/K-ATPases (FITC−H/K-ATPase) were examined. The fluorescence probe FITC binds to a Lys residue (in the case of pig gastric H/K-ATPase at Lys-518) which is embedded in the ATP binding domain of P-type ATPases (*7*, *36*, *39*). The resulting preparation loses its ATPase activity almost completely with no detectable loss in K^+-dependent *p*-nitrophenylphosphatase activity. The amount of bound FITC (4.9 nmol/mg) was twice as large as that of EP formed from ATP (2.5 nmol/mg), namely, around 1 mol of FITC probe/mol of α-chain. The images obtained were morphologically similar to those from native H/K-ATPase. When an anti-FITC antibody was complexed with 1-ethyl-3-(3-dimethylaminopropyl)carbodimide prior to solubilization, antibody-bound images were clearly observed (Figure 1D). However, such images were not found when the native enzyme was used (not shown). These data indicate that H/K-ATPase molecules also have protomeric and oligomeric structures as has previously been observed for Na/K-ATPase (*25*).

Table 1: Enzymatic Activity of Detergent-Solubilized H/K-ATPases[a]

	membrane-bound	$C_{12}E_8$	nOG
v, μmol of P_i/mg/h	125 ± 1.3	2.2 ± 1.6	88.6 ± 2.5
EP, nmol/mg	2.52 ± 0.04	0.11 ± 0.16	1.74 ± 0.06
TN, s^{-1}	13.8 ± 0.21	*b*	14.1 ± 0.40

[a] $C_{12}E_8$- and nOG-solubilized H/K-ATPase was assayed for H/K-ATPase activity (v) and EP at 25 °C, pH 5.5. Turnover numbers (v/EP, TN) were estimated. [b] It was not possible to estimate the turnover number because enzymatic activities were not detectable within experimental error.

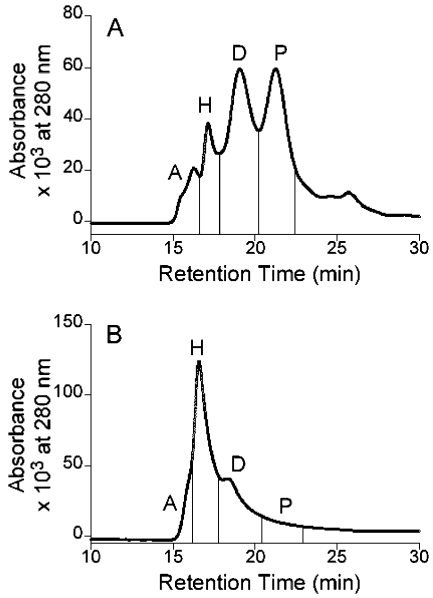

FIGURE 2: Elution profile of solubilzied H/K-ATPase by high-performance gel chromatography. (A) $C_{12}E_8$-solubilized H/K-ATPases and (B) nOG-solubilized H/K-ATPase preparations were subjected to HPGC with a TSKgel G3000SW_{XL} column at 0 °C. The absorbance at 280 nm was monitored with a diode array detector and recorded. The solubilized H/K-ATPase was separated into the four fractions of aggregate (A), higher oligomer (H), diprotomer (D), and protomer (P).

Gel Chromatographic Separations of Oligomeric Species of H/K-ATPase Solubilized with Detergents. To assess the distribution of oligomeric species of $C_{12}E_8$-solubilized H/K-ATPase, which showed very low H/K-ATPase activity and phosphorylation capacity (Table 1), oligomeric H/K-ATPases were separated by HPGC (Figure 2A). When the $C_{12}E_8$-solubilized H/K-ATPase was applied to the column, four major protein fractions appeared, an aggregate (A), higher oligomers (H), diprotomers (D), and a protomer (P), as observed in the case of Na/K-ATPase (*40*−*42*). Fraction A was too large to permit an estimation of molecular weight (void volume of the column). The molecular weight of fraction H was estimated to be larger than that of the $(\alpha\beta)_2$-diprotomer. The molecular weights of the $\alpha\beta$-protomer and the $(\alpha\beta)_2$-diprotomer were estimated to be approximately 1.5×10^5 and 3.0×10^5, respectively (*18*, *40*). The relative amount of H, D, and P was calculated to be 12%, 44%, and 44% of the total enzymes, respectively (Table 2).

To investigate structure−activity relationships, an active soluble H/K-ATPase is a prerequisite. Several detergents can be used to solubilize H/K-ATPase (*9*, *15*, *43*, *44*). In the

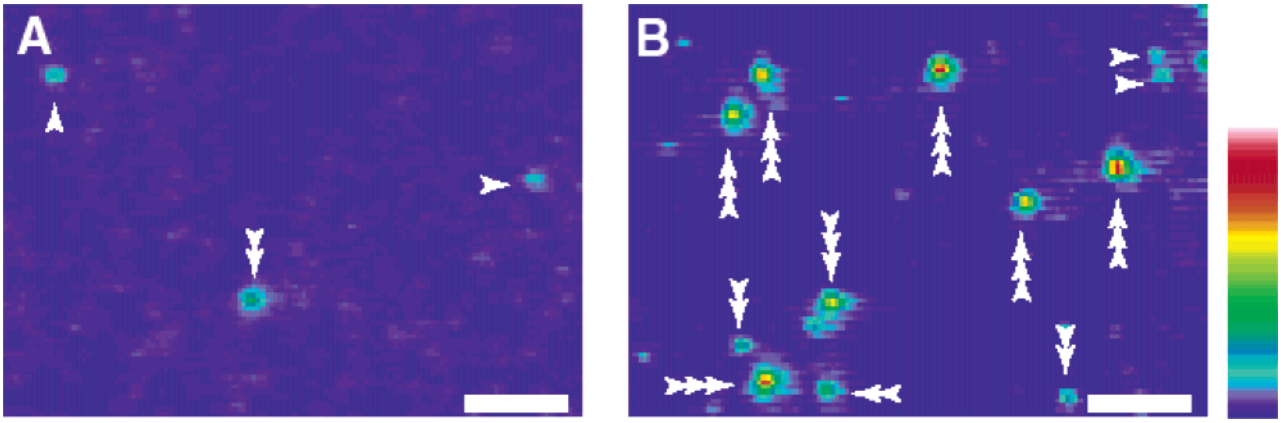

FIGURE 3: Pseudocolor displays of fluorescence images of FITC-modified H/K-ATPase molecules. FITC-modified H/K-ATPase was solubilized by (A) $C_{12}E_8$ and (B) nOG, and observed by TIRFM. The image constituted 10 integrated video frames just after laser illumination to reduce noise. The initial fluorescence intensities with one, two, and four units are indicated by single, double, and triple arrowheads, respectively. A scale bar of 5 μm and a linear 0−255 pseudocolor scale of fluorescence intensity are shown.

Table 2: Comparison of the Distribution of Oligomers in Detergent-Solubilized H/K-ATPase, As Estimated by TIRFM and HPGC Analysis[a]

	HPGC (%)			TIRFM (%)		
	P	D	H	P	D	T
$C_{12}E_8$	44	44	12	51	44	5
nOG	10	34	56	0	46	54

[a] The composition of oligomeric species of $C_{12}E_8$- or nOG-solubilized H/K-ATPase determined by HPGC was calculated as the relative area of the UV absorbance of each fraction, and that by TIRFM was calculated as the total protomers (the area of each Gaussian curve times the number of oligomers). The values indicate the percentages of protomer, diprotomer, and higher oligomer (in HPGC analysis) or tetraprotomer (in TIRFM analysis), respectively. In each case, the sum of each protomer was set as 100%. The specific activities of the $C_{12}E_8$- and nOG-solubilized H/K-ATPaes calculated as the percentage of membrane-bound enzyme are 1.8% and 71%, respectively.

present investigations, nOG proved to be useful for solubilization without significant inactivation of the H/K-ATPase activity, as has been previously reported (*44*). When membrane-bound H/K-ATPase was solubilized with 2% (w/v) nOG, the specific activity of the supernatant fraction was approximately 71% of that of the membrane-bound H/K-ATPase preparations, retaining the same turnover number (v/EP) of the membrane H/K-ATPase (Table 1). The result of the HPGC analysis of nOG-solubilized H/K-ATPase showed a large increase in the proportion of fraction H and a decrease in those of D and especially P (Figure 2B) compared with the case of $C_{12}E_8$-solubilized H/K-ATPase (Figure 2A). The relative amount of each fraction was found to be 56%, 34%, and 10% for H, D, and P, respectively (Table 2).

Single-Molecule Observation of FITC−H/K-ATPase Molecules in Solution. Assemblies of the enzyme are on the scale of nanometers, so it would be impossible to observe each individual molecule in an aqueous solution by optical microscopy. A single fluorophore attached to the protein can be clearly observed in an aqueous solution by fluorescent microscopy using an evanescent field produced when a laser beam is totally reflected in the interface between the water and glass (*37*, *45*−*49*). Using total internal reflection fluorescent microscopy (TIRFM), it would be possible to directly count the number of FITC-modified protomeric molecules that are assembled. Namely, the fluorescence intensity of diprotomeric or tetraprotomeric FITC−H/K-ATPase is 2 or 4 times as large as that of the protomeric one. To determine how many protomers are assembled in the higher oligomers detected by HPGC analysis, we modified the enzyme with FITC at Lys-518 as described above (*7*, *36*, *39*) and subjected the detergent-solubilized FITC−H/K-ATPases to a TIRFM analysis.

Figure 3 shows the fluorescence images of FITC−H/K-ATPase on the surface of a coverslip. An approximately 10 pM concentration of detergent-solubilized FITC−H/K-ATPase could easily be detected as individual fluorescent spots with various fluorescence intensities in an illumination field of approximately 60 × 60 μm^2. The number of fluorescent spots was proportional to the applied FITC−H/K-ATPase concentration (except when FITC−HK-ATPase was extremely diluted to sub-picomolar levels). Only a few spots were observed in the buffer or unmodified samples (not shown) Thus, we conclude that the effect of dust particles was negligible in this analysis, and that the fluorescent spots were largely due to the FITC probe bound to the enzyme.

As a control experiment, FITC−H/K-ATPase was solubilized with SDS to completely dissociate the $\alpha\beta$-protomer of H/K-ATPase into α- and β-chains. Figure 4A shows a typical example of the single-step photobleaching of the FITC probe for a single molecule (*45*) observed in almost every spot of the SDS-solubilized FITC-bound α-chain. The sum of the fluorescence trajectories of over 100 spots (Figure 4D, open circles) resulted in a single-exponential curve with a rate of 1.03 s^{-1}, comparable to that obtained in ensemble experiments. The initial intensity of each fluorescent spot gave a single peak that fitted well to a single Gaussian distribution with a mean intensity of 9.6. We therefore conclude that, with a single-step photobleaching, the spots represent images of single molecules (Figure 5A).

In the case of $C_{12}E_8$-solubilized FITC−H/K-ATPase, not only the single FITC probe but two and more FITC probes in one particle were also observed. The fluorescence trajectories of spots showed mainly a one-step and a two-step (Figure 4B) quantized photobleaching. Figure 5B shows the distribution of fluorescence intensities of $C_{12}E_8$-solubilized FITC−H/K-ATPase. The intensity distribution could be fitted to two main component Gaussian curves; one major

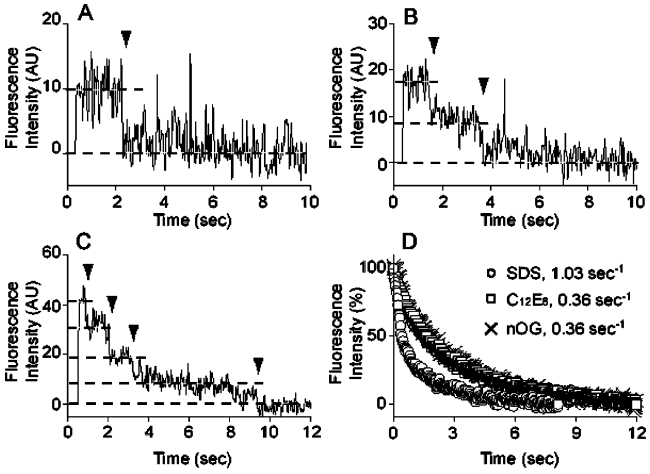

FIGURE 4: Fluorescence trajectories of single particles at the video rate. Typical quantitized photobleaching with one (A), two (B), and four (C) step(s) is shown. The background intensity (the average intensity of 150 video frames 15 s after laser illumination) was set as zero. Photobleaching occurred at the times indicated by the arrowheads. (D) The exposure time for photobleaching was measured for more than 100 single particles, and the data are summarized and plotted as a function of time. The decay could be fitted to a single-exponential function.

curve was indistinguishable from that of SDS-solubilized FITC−H/K-ATPase with a mean intensity of 8.9. The mean intensity of the other was twice that of the major one, which can be attributed to the presence of diprotomeric molecules. In addition, a very minor curve with a 4-fold larger mean intensity, which can be attributed to tetraprotomeric molecules, was also found. The distribution of protomers (P), diprotomers (D), and tetraprotomers (T) was calculated (the area of each Gaussian curve times the number of oligomers) to be 51%, 44%, and 5%, respectively (Table 2).

In the case of the nOG-solubilized FITC−H/K-ATPase, the number of bright spots increased considerably (Figure 3B). Spots with both four steps and two steps appeared with a few one-step photobreaching spots (Figure 4B,C). The distribution of fluorescence intensities in nOG-solubilized FITC−H/K-ATPase consisted of two major Gaussian curves, corresponding to double and quadruple fluorophores, assuming the mean intensity of the single fluorophore to be 9.1 (Figure 5C). The distribution of D and T was calculated to be 46% and 54%, respectively (Table 2). From these results, we conclude that the higher oligomer fraction observed by HPGC analysis corresponds to a tetraprotomer.

Figure 4D shows a measurement of the exposure time required to achieve photobleaching. The photobleaching of individual fluorophores was a stochastic process, and the integrals of the fluorescence trajectories of the individual spots of each detergent-solubilized preparations were fitted to a single-exponential function with a pseudo-first-order rate constant of 1.03, 0.36, and 0.36 s^{-1}, respectively. The difference in the rate constant for photobleaching between the SDS-solubilized sample and the $C_{12}E_8$- or nOG-solubilized samples may reflect the difference in the unfolding of the ATP binding pocket containing the FITC probe (*7*) due to the accessibility of oxygen radicals to the exposed fluorophore.

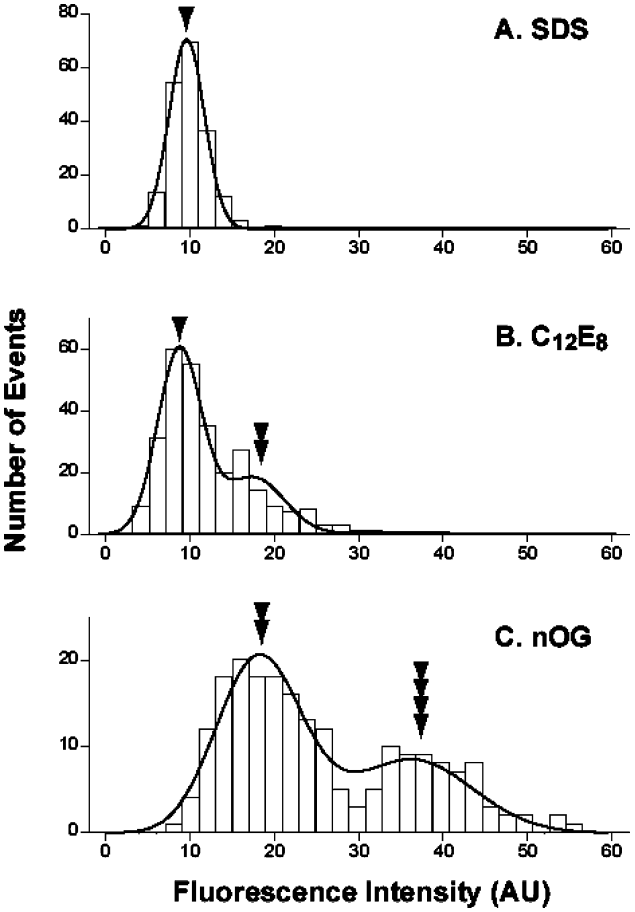

FIGURE 5: Histogram of the fluorescence intensity of solubilized H/K-ATPase. Distributions of fluorescence intensities of FITC−H/K-ATPase solubilized with SDS (A, $n = 189$), $C_{12}E_8$ (B, $n = 283$), and nOG (C, $n = 206$) are shown. Fluorescence intensities of independent spots, which showed stepwise photobleaching, at a five-video-frame average just after laser illumination were achieved. The background intensity was subtracted, as in Figure 4. The fluorescence intensities of one to four dye molecules were in the linear range of the camera. The data were fitted to Gaussian curves; $\sum C_i \exp[-(x - iM)^2/2i\sigma^2]$, where i (=1−4) is the number of Gaussian curves, C_i, M, and σ are fitting parameters, and x is fluorescence intensity. The solid line indicates the sum of one to four Gaussian components fitted to the data. Single, double, and quadruple arrowheads indicate the peak positions of each Gaussian distribution which is responsible for one, two, or four fluorescence molecules, respectively.

DISCUSSION

The oligomeric states of pig gastric H/K-ATPase preparations were characterized by several independent methods. Our previous report, based on the presence of 0.5 mol of EP and 0.5 mol of EATP/mol of α-chain of membrane-bound enzymes, suggested the presence of a 2*n*-mer as the functional unit of the enzyme (*12*, *17*).

Electron microscopic observation of rotary-shadowed molecules of H/K-ATPase solubilized by $C_{12}E_8$ showed the presence of protomeric, diprotomeric, and higher oligomeric structures, as in the case of Na/K-ATPase (*25*), which has a structure homologous to that of H/K-ATPase (*1*−*4*). When $C_{12}E_8$-solubilized H/K-ATPases were separated by gel filtration as described above, electron microscopic images indicated the presence of a protomer, diporotomers, and higher oligomerers in all fractions (data not shown). These data can be taken to indicate the existence of a slow equilibrium

between oligomers in solution, since more than 2 h is required for the fixation and observation of H/K-ATPase molecules at room temperature. The solubilization of active H/K-ATPase using $C_{12}E_8$ at 5 °C has been reported (*15*). However, further studies are required to obtain an active solubilized H/K-ATPase with $C_{12}E_8$ at room temperature as in the case of other P-type ATPases (*31*, *42*).

The HPGC separation of inactivated $C_{12}E_8$-solubilized H/K-ATPase and of active nOG-solubilized H/K-ATPase permitted us to characterize and quantify the diprotomer and protomer. The correlation between the amount of fraction H and the specific activity of detergent-solubilized H/K-ATPase retaining the same turnover number as the membrane-bound enzyme suggests that the higher oligomer is the active species (Table 2, HPGC). Fraction A contained around 6% of the UV absorption in both inactive $C_{12}E_8$- and active nOG-solubilized H/K-ATPase. This suggests that fraction A contains impurities and/or inactive aggregated H/K-ATPase. Negligible ATPase activity and ATP binding were reported in fraction A of Na/K-ATPase (*42*).

To characterize the high molecular weight fraction, FITC−H/K-ATPase was examined by TIRFM, which has recently been developed for observing single fluorescent molecules in solution (*37*, *45*−*49*). The advantage of single-molecule studies is that they provide information on the dynamics of complex macromolecules at the level of individual molecules, which are masked in ensemble-averaged experiments. TIRFM would be a useful method for the detection of single fluorescent molecule characteristics because of its lower background. We were able to characterize the relative fluorescence intensity and photobleaching of the FITC probe at Lys-518. This process is quantized in a manner typical of single molecules. We were also able to directly count the number of FITC-labeled H/K-ATPase catalytic subunits. This represents the first observation of a single molecule of P-type ATPase in an aqueous solution, which may also be useful for determining higher oligomeric structures of other P-type ATPases. The distribution of the initial intensity of the FITC fluorescence of $C_{12}E_8$-solubilized and nOG-solubilized FITC−H/K-ATPase, respectively, indicated that protomers + diprotomers and diprotomers + tetraprotomers are the main species (Table 2, TIRFM). The TIRFM measurements, which showed the higher oligomer in HPGC to be a tetraprotomer, and the distribution of oligomeric states examined by two methods are rather close to each other as shown in Table 2. The turnover number of the nOG-solubilized enzyme is nearly the same as that of the membrane-bound enzyme (Table 1).

Although more quantitative experiments are required, the above data suggest that the main reason for the 30% reduction in the specific activity of nOG-solubilized H/K-ATPase may be related to the appearance of a diprotomer and a protomer fraction as determined by HPGC (Table 2), which may also be related to the delipidation required for H/K-ATPase activity (*50*). In the case of Na/K-ATPase, the importance of acidic phospholipids, not only in ATPase activity, but also in the association of $\alpha\beta$-protomers, has been demonstrated (*18*, *51*, *52*). The fact that both $C_{12}E_8$- and nOG-solubilized FITC−H/K-ATPase showed nearly the same rate constant for the photobleaching of the FITC probe may exclude the possibility that the unfolding of the ATP binding pocket occurs as in the case of the SDS-inactivated enzyme. The presence of a slow equilibrium between oligomers was indicated by electron microscopic observation, as described above, which might be the reason for the differences between the specific activity and the amount of tetraprotomer detected by HPGC and/or TIRFM in each nOG-solubilized and $C_{12}E_8$-solubilized H/K-ATPase. These considerations suggest that the tetraprotomeric form rather than diprotomeric or protomeric form of H/K-ATPase molecules is the functional component in the membrane, although there appear to be long-standing debates concerning the structure of P-type ATPase, namely, whether a protomer is the functional unit of the enzyme (*53*−*58*) or an oligomer is required (*16*−*31*, *42*, *59*). The protomeric and diprotomeric forms of nOG-solubilized-H/K-ATPase appeared to be inactive, as described above. However, the specific activity of the tetraprotomer in Na/K-ATPase was reported to be nearly the same as that of the membrane-bound enzyme but approximately half that of the diprotomer and protomer (*42*). Thus, the important point is that the turnover number of each soluble tetraprotomer of these two ATPases was rather close to that of the membrane-bound enzyme. These data suggest that the tetraprotomer is the functional unit of H/K-ATPase and Na/K-ATPase in the membrane, both of which showed half of the site reactivity and all of the site reactivity, depending on the ligands present (*12*, *16*, *17*, *54*).

The characterization of the cross-linking domain of H/K-ATPase (*13*) and Na/K-ATPase (*20*) suggests that the protomer can associate between the cytoplasmic domains. $C_{12}E_8$-solubilized Na/K-ATPase has been reported to bind to the synthetic polypeptide of the His_6-tagged large cytoplasmic loop (M4−M5) of Na/K-ATPase in the presence of MgATP (*60*). These data point to the possibility that the large cytoplasmic domains interact with each other, which is consistent with our previous report of half-site phosphorylation and half-site ATP binding in both ATPases (*17*, *25*). The identification of interaction domains (or interfaces) between protomers will be necessary to obtain a picture of how these pump molecules function.

ACKNOWLEDGMENT

We thank Drs. K. Sakaguchi, H. Kojima, and T. Nishizaka for critical discussion, Mr. T. Takeguchi for analysis of a single molecule, and Ms. Y. Momose for secretarial assistance in preparing this manuscript.

REFERENCES

1. Rabon, E. C., and Reuben, M. A. (1990) *Annu. Rev. Physiol. 52*, 321−344.
2. Klaassen, C. H. W., and De Pont, J. J. H. H. M. (1994) *Cell. Physiol. Biochem. 4*, 115−134.
3. Hersey, S. G., and Sachs, G. (1995) *Physiol. Rev. 75*, 155−189.
4. Shull, G. E., Schwarz, A., and Lingrel, J. B. (1985) *Nature 316*, 691−695.
5. Maclennan, D. H., Brandl, C. J., Korczak, B., and Green, M. (1985) *Nature 316*, 696−700.
6. Shull, G. E., and Lingrel, J. B. (1986) *J. Biol. Chem. 261*, 16788−16791.
7. Toyoshima, C., Nakasako, M., Nomura, H., and Ogawa, H. (2000) *Nature 405*, 647−655.
8. Toyoshima, C., and Nomura, M. (2002) *Nature 418*, 605−611.
9. Soumarmon, A., Robert, J. C., and Lewin, M. J. M. (1986) *Biochim. Biophys. Acta 860*, 109−117.
10. Rabon, E. C., Gunther, R. D., Bassilan, S., and Kempner, E. S. (1988) *J. Biol. Chem. 263*, 16189−16194.

11. Hebert, H., Xian, Y., Hacksell, I., and Mardh, S. (1992) *FEBS Lett. 299*, 159−162.
12. Eguchi, H., Kaya, S., and Taniguchi, K. (1993) *Biochem. Biophys. Res. Commun. 196*, 294−300.
13. Shin, J. M., and Sachs, G. (1996) *J. Biol. Chem. 271*, 1904−1908.
14. Morii, M., Hayata, Y., Mizoguchi, K., and Takeguchi, N. (1996) *J. Biol. Chem. 271*, 4068−4072.
15. Lacapere, J. J., Robert, J. C., and Soumarmon, A. T. (2000) *Biochem. J. 345*, 239−245.
16. Taniguchi, K., Kaya, S., Abe, K., and Mårdh, S. (2001) *J. Biochem. (Tokyo) 129*, 335−342.
17. Abe, K., Kaya, S., Imagawa, T., and Taniguchi, K. (2002) *Biochemistry 41*, 2438−2445.
18. Mimura, K., Matsui, H., Takagi, T., and Hayashi, Y. (1993) *Biochim. Biophys. Acta 1145*, 63−74.
19. Ganjeizadeh, M., Zolotarjova, N., Huang, W. H., and Askari, A. (1995) *J. Biol. Chem. 270*, 15707−15710.
20. Sarvazyan, N. A., Modyanov, N. N., and Askari, A. (1995) *J. Biol. Chem. 270*, 26528−26532.
21. Thönges, D., Linnertz, H., and Schoner, W. (1997) *Ann. N. Y. Acad. Sci. 834*, 322−326.
22. Tsuda, T., Kaya, S., Yokoyama, T., Hayashi, Y., and Taniguchi, K. (1998) *J. Biol. Chem. 273*, 24334−24338.
23. Linnertz, H., Urbanova, P., Obsil, T., Herman, P., Amler, E., and Schoner, W. (1998) *J. Biol. Chem. 273*, 28813−28821.
24. Anatolovic, R., Hamer, E., Serpersu, E. H., Kost, H., Linnertz, H., Kovarik, Z., and Schoner, W. (1999) *Eur. J. Biochem. 261*, 181−189.
25. Yokoyama, T., Kaya, S., Abe, K., Taniguchi, K., Katoh, T., Yazawa, M., Hayashi, Y., and Mårdh, S. (1999) *J. Biol. Chem. 274*, 31792−31796.
26. Askari, A. (2000) in *Na/K-ATPase and Related ATPases* (Taniguchi, K., and Kaya, S., Eds.) pp 17−26, Elsevier Science, Amsterdam, The Netherlands.
27. Donnet, C., Arystarkhova, E., and Sweadner, K. (2001) *J. Biol. Chem. 276*, 7357−7365.
28. Ivanov, A. V., Modyanov, N. N., and Askari, A. (2002) *Biochem. J. 364*, 293−299.
29. Froehlich, J. P., Taniguchi, K., Fendler, K., Mahaney, J. E., Thomas, D. D., and Albers, R. W. (1997) *Ann. N. Y. Acad. Sci. 834*, 280−296.
30. Nakamura, S., Suzuki, H., and Kanazawa, T. (1997) *J. Biol. Chem. 272*, 6232−6237.
31. Nakamura, J., Tajima, G., Sato, C., Furukohri, T., and Konishi, K. (2002) *J. Biol. Chem. 277*, 24180−24190.
32. Chang, H., Saccomani, G., Rabon, E., Schackmann, R., and Sachs, G. (1977) *Biochim. Biophys. Acta 464*, 313−327.
33. Yeh, L., Cosgrove, P., and Holt, W. F. (1990) *Membr. Biochem. 9*, 129−140.
34. Bradford, M. M. (1976) *Anal. Biochem. 72*, 248−254.
35. Carilli, C. T., Farley, R. A., Perlman, D. M., and Cantley, L. C. (1982) *J. Biol. Chem. 257*, 5601−5606.
36. Jackson, R. J., Mendlein, J., and Sachs, G. (1983) *Biochim. Biophys. Acta 731*, 9−15.
37. Oiwa, K., Eccleston, J. F., Anson, M., Kikumoto, M., Davis, C. T., Reid, G. P., Ferenczi, M. A., Corrie, J. E. T., Yamada, A., Nakayama, H., and Trentham, D. R. (2000) *Biophys. J. 78*, 3048−3071.
38. Ohara-Imaizumi, M., Nakamichi, Y., Nishiwaki, C., and Nagamatsu, S. (2002) *J. Biol. Chem. 277*, 50805−50811.
39. Farley, R. A., and Faller, L. D. (1985) *J. Biol. Chem. 260*, 3899−3901.
40. Hayashi, Y., Mimura, K., Matsui, H., and Takagi, T. (1989) *Biochim. Biophys. Acta 983*, 217−229.
41. Hayashi, Y., Kobayashi, T., Shinji, N., Hagiwara, E., Tahara, Y., and Takenaka, H (2000) in *Na/K-ATPase and Related ATPases* (Taniguchi, K., and Kaya, S., Eds.) pp 357−364, Elsevier Science, Amsterdam, The Netherlands.
42. Hayashi, Y., Shinji, N., Tahara, Y., Hagiwara, E., and Takenaka, H. (2003) *Ann. N. Y. Acad. Sci. 986*, 232−234.
43. Soumarmon, A., Grelac, F., and Lewin, M. J. M. (1983) *Biochim. Biophys. Acta 732*, 579−585.
44. Rabon, E., Guanther, R. D., Soumarmon, A., Bassillian, S., Lewin, M., and Sachs, G. (1985) *J. Biol. Chem. 260*, 10200−10207.
45. Funatsu, Y., Harada, Y., Tokunaga, M., and Yanagida, T. (1995) *Nature 374*, 555−559.
46. Nie, S., and Zare, R. N. (1997) *Annu. Rev. Biophys. Biomol. Struct. 26*, 567−596.
47. Xie, S. X., and Trautman, J. K. (1998) *Annu. Rev. Phys. Chem. 49*, 437−476.
48. Ha, T., Ting, A. Y., Liang, J., Caldwell, W. B., Deniz, A. A., Chemla, D. S., Schultz, P. G., and Weiss, S. (1999) *Proc. Natl. Acad. Sci. U.S.A. 96*, 893−898.
49. Tokunaga, M., Kitamura, K., Iwane, A. H., and Yanagida, T. (1997) *Biochem. Biophys. Res. Commun. 235*, 47−53.
50. Nandi, J., Wright, M. V., and Ray, T. K. (1983) *Biochemistry 22*, 5814−5821.
51. Wheeler, K. P., and Whittam, R. (1970) *J. Physiol. 207*, 303−328.
52. Taniguchi, K., and Tonomura, Y. (1971) *J. Biochem. (Tokyo) 69*, 543−557.
53. McIntosh, D. H. (1988) *Adv. Mol. Cell. Biol. 23A*, 33−99.
54. Martin, D. W., and Sachs, J. R. (1999) *Biochemistry 38*, 7485−7497.
55. Martin, D. W., Marecek, J, Scarlata, S, and Sachs, J. R. (2000) *Proc. Natl. Acad. Sci. U.S.A. 97*, 3195−3200.
56. Vilsen, B., Andersen, J. P., and Jorgensen, P. L. (1987) *J. Biol. Chem. 262*, 10511−10517.
57. Jorgensen, P. L., Håkansson, K. O., and Karlish, S. J. D. (2003) *Annu. Rev. Physiol. 65*, 817−849.
58. Ward, D. G. and Cavieres, J. D. (2003) *J. Biol. Chem. 278*, 14688−14697.
59. Teramachi, S., Imagawa, T., Kaya, S., and Taniguchi, K. (2002) *J. Biol. Chem. 277*, 37394−37400.
60. Costa, C. J., Gatto, C., and Kaplan, J. (2003) *J. Biol. Chem. 278*, 9176−9184.

BI035686X